

Deformation Time-Series of the Lost-Hills Oil Field using a Multi-Baseline Interferometric SAR Inversion Algorithm with Finite-Difference Smoothing Constraints

Charles Werner, Tazio Strozzi and Urs Wegmüller
Gamma Remote Sensing AG, Worbstrasse 225, Gümligen, Switzerland
cw@gamma-rs.ch +41 31 951-7005

Introduction

The Lost-Hills oil field located in Kern County, California ranks sixth in total remaining reserves in California. Hundreds of densely packed wells characterize the field with one well every 5000 to 20000 square meters. Subsidence due to pumping of oil is up to 20 cm/year and is highly variable both in space and time. The RADARSAT-1 satellite collected Fine-Beam 1 SAR data over this area with a 24-day repeat during a 2 year period spanning 2002-2004. A total of 28 scenes were used in this study. Relatively high Interferometric SAR correlation makes this an excellent region for development and test of **deformation time-series** inversion algorithms.

Problem Definition

Errors in deformation time series derived from a stack of differential interferograms are due to **errors** in the **digital terrain model**, **Interferometric baselines**, **variability in tropospheric delay**, thermal noise and **phase unwrapping** errors. Particularly challenging is the **separation of non-linear deformation**, from **path delay due to troposphere**, and **phase unwrapping errors**.

In **Figure 2** we show the network of 40 interferograms selected from pairs of Radarsat-1 acquisitions based on the criterion of perpendicular baselines between 100 and 400 meters and time intervals between 23 and 144 days. Each line represents a single interferogram. The numbers refer to entries in the table of 28 SLCs used to form the network. Note that there are no isolated nodes. **Figure 3** shows a montage of the set of phase unwrapped interferograms. Regions of low interferometric correlation have been masked out after unwrapping using the Minimum Cost Flow, (Constantini, 1998).

Proposed Solution

Based on an extension of the SVD based Least-Squares inversion as described by Lee et al. (2010), Schmidt and Bürgmann (2003), and the earlier work of Berardino (2002), our algorithm combines estimation of the DEM height error with a set of finite difference smoothing constraints. A set of linear equations are formulated for each spatial point that are functions of the deformation velocities during the time intervals spanned by the interferogram and a DEM height correction. The sensitivity of the phase to the height correction depends on the perpendicular baseline component of each interferogram.

This design matrix (**Figure 4**) is augmented with a set of additional weighted constraints on the acceleration of the surface that penalize rapid velocity variations. The weighting factor γ can be varied from 0 (no smoothing) to a large values (> 10) that yield time-series solutions that are essentially linear. The factor can be tuned to take into account a priori knowledge of the deformation non-linearity and coherence.

Gaps in the interferometric time series manifest as singular values close to 0. Forcing these to 0.0 leads to a stable inversion for the deformation rates v_i and height correction h . Setting the smoothing constraint to zero results in zero deformation rate during any time periods not covered by the network. Adding the constraints leads to smooth velocity changes. The deformation time series is obtained by integrating the velocities in the solution. Figure 5 shows the deformation history at single location for different values of γ .

Our analysis shows non-linear deformation related to changes in the extraction as well as height corrections consistent with the 3-arc-sec SRTM DEM that are relatively insensitive to γ as shown in Figures 6-7.

Conclusions

- Demonstrated Least-Squares algorithm solving multi-reference interferometric stack for smoothed time-series and height
- Constraint parameter γ permits adjusting the degree of smoothing for **linear and non-linear deformation**
- Height corrections relatively independent of the smoothing parameter value
- Reasonable solution also for non-fully connected networks
- Least-Squares error is useful to detect phase-unwrapping errors

References and Acknowledgements

P. Berardino, G. Fornaro, R. Lanari, and E. Sansosti, "A new algorithm for surface deformation monitoring based on small baseline differential SAR interferograms," IEEE Trans. Geosci. Remote Sens., vol. 40, no. 11, pp. 2375-2383, Nov. 2002.
M. Constantini, "A Novel Phase-Unwrapping Algorithm based on Network Programming," IEEE Trans. Geosci. Remote Sens., vol. 36, no. 3, pp. 813-820, May, 1998
D. A. Schmidt and R. Bürgmann, "Time-dependent land uplift and subsidence in the Santa Clara valley, California from a large InSAR data set," J. Geophys. Res., vol. 108, no. B9, p. 2416, Sep. 2003, DOI: 10.1029/2002JB002267
C.W, Lee, Z. Lu, H-S Jung, J-S Wong, and D. Dzurisin, "The 2006 Eruption of Augustine Volcano, Alaska", Chapter 18, U.S. Geological Survey Professional Paper 1769, 2010. <http://pubs.usgs.gov/pp/1769>.

Thanks to David Schmidt for very helpful discussions concerning the data analysis in the 2003 paper published with Roland Bürgmann on Santa Clara Valley deformation.



Figure 1. Belridge, California oil field

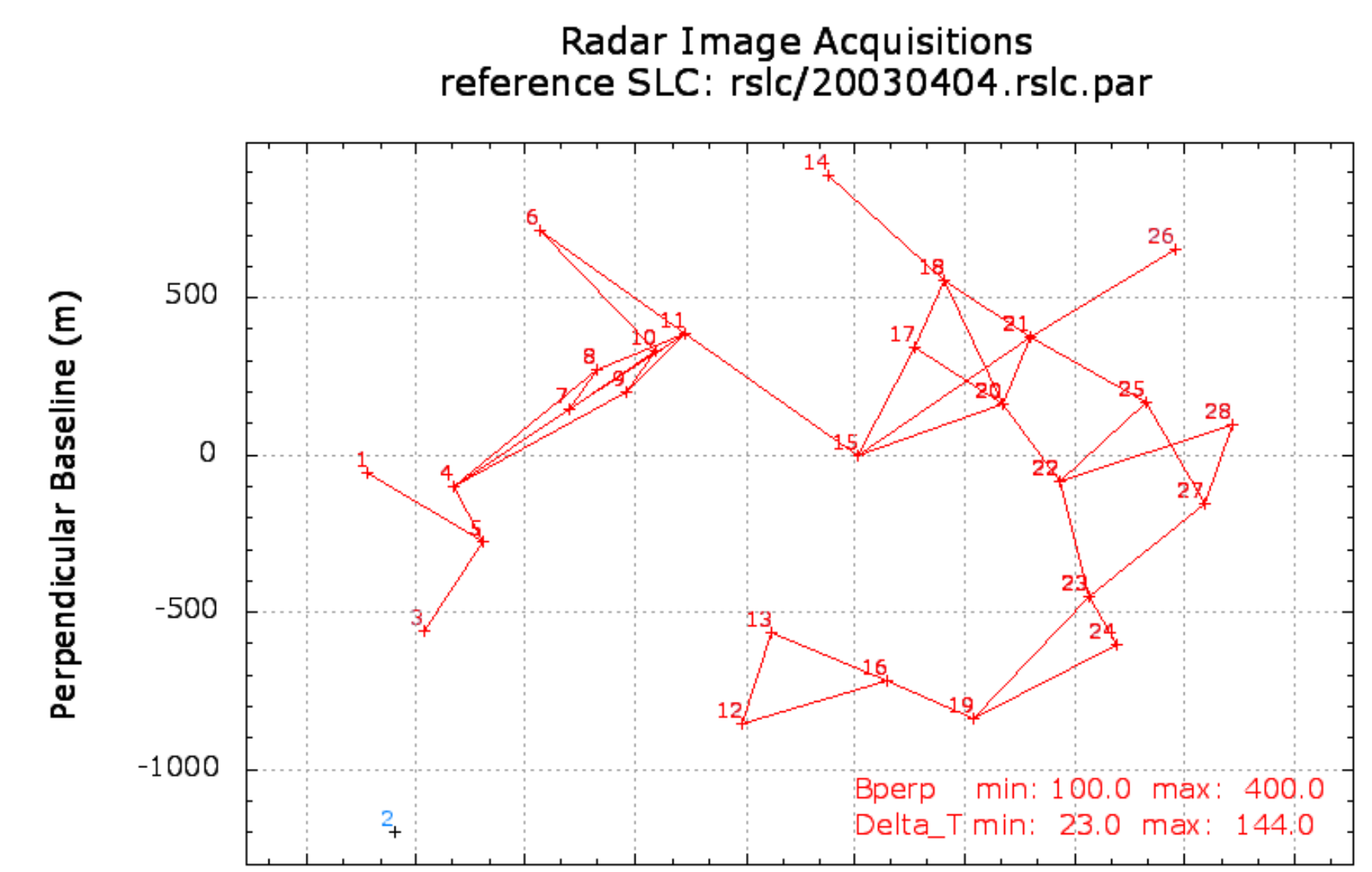


Figure 2. Time Series Interferogram Network



Figure 3. Unwrapped interferograms showing atmosphere and deformation phase

$$\begin{bmatrix} T_0 & T_1 & T_2 & T_3 & T_4 & \frac{\partial \phi_0}{\partial h} \\ 0 & T_1 & T_2 & 0 & 0 & \frac{\partial \phi_1}{\partial h} \\ 0 & 0 & T_2 & T_3 & T_4 & \frac{\partial \phi_2}{\partial h} \\ T_0 & T_1 & T_2 & T_3 & 0 & \frac{\partial \phi_3}{\partial h} \\ 0 & 0 & 0 & T_3 & T_4 & \frac{\partial \phi_4}{\partial h} \\ 0 & 0 & T_2 & T_3 & 0 & \frac{\partial \phi_5}{\partial h} \\ \gamma^2 & -2\gamma^2 & \gamma^2 & 0 & 0 & 0 \\ 0 & \gamma^2 & -2\gamma^2 & \gamma^2 & 0 & 0 \\ 0 & 0 & \gamma^2 & -2\gamma^2 & \gamma^2 & 0 \end{bmatrix} \begin{bmatrix} v_0 \\ v_1 \\ v_2 \\ v_3 \\ v_4 \\ h \\ 0 \\ 0 \\ 0 \end{bmatrix} = \begin{bmatrix} \phi_0 \\ \phi_1 \\ \phi_2 \\ \phi_3 \\ \phi_4 \\ \phi_5 \\ 0 \\ 0 \\ 0 \end{bmatrix} \quad \Psi_0 = 0.0 \quad \Psi_i = \sum_{j=0}^i v_j T_j$$

Figure 4. Least-Squares formulation for a single point in a stack of 6 interferograms. The observed phases are the ϕ_i . The deformation velocities for the 5 epochs are v_i . The values of the T_i is time intervals in days between epochs. The additional constraints in the lower 3 rows add cost when the velocity changes. The additional column of the design matrix contains the sensitivity of the phase w.r.t height and is proportional to the perpendicular component of the baseline. The total time series phase Ψ_i at each epoch is obtained by summing the incremental deformation for each interval T_i .

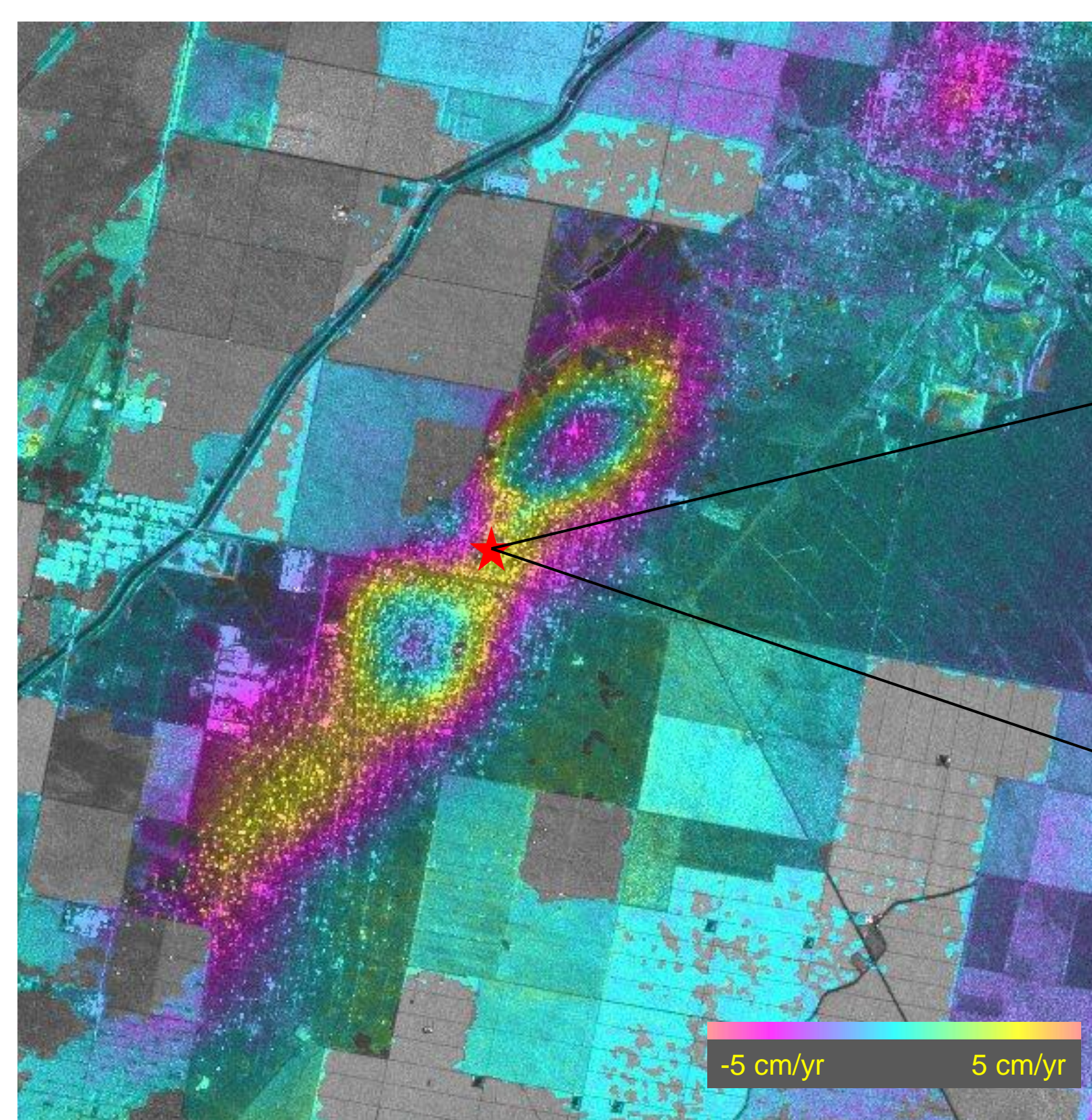


Figure 5. Average Deformation rate over two years. Deformation histories for $\gamma = 1, 10$

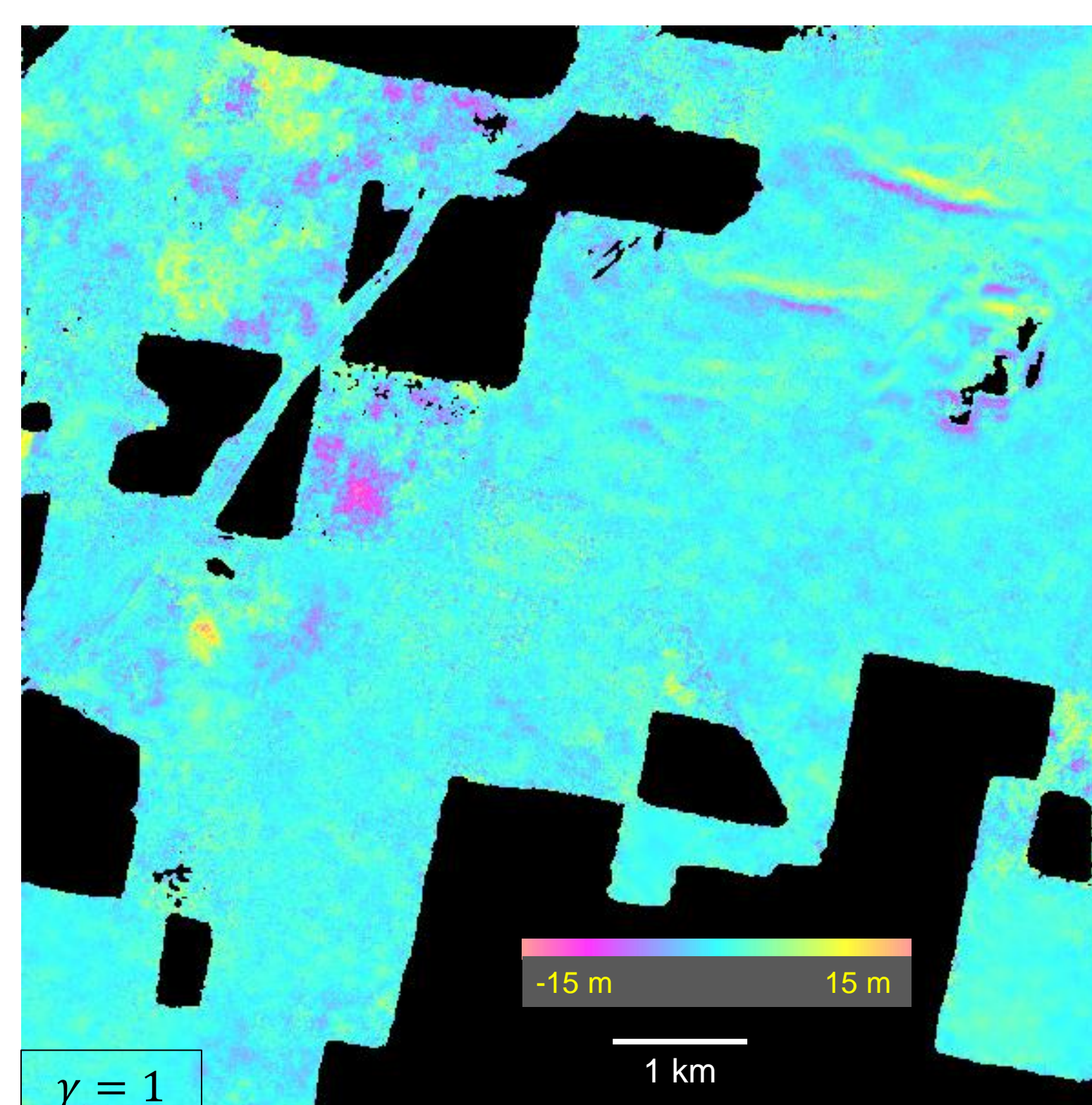
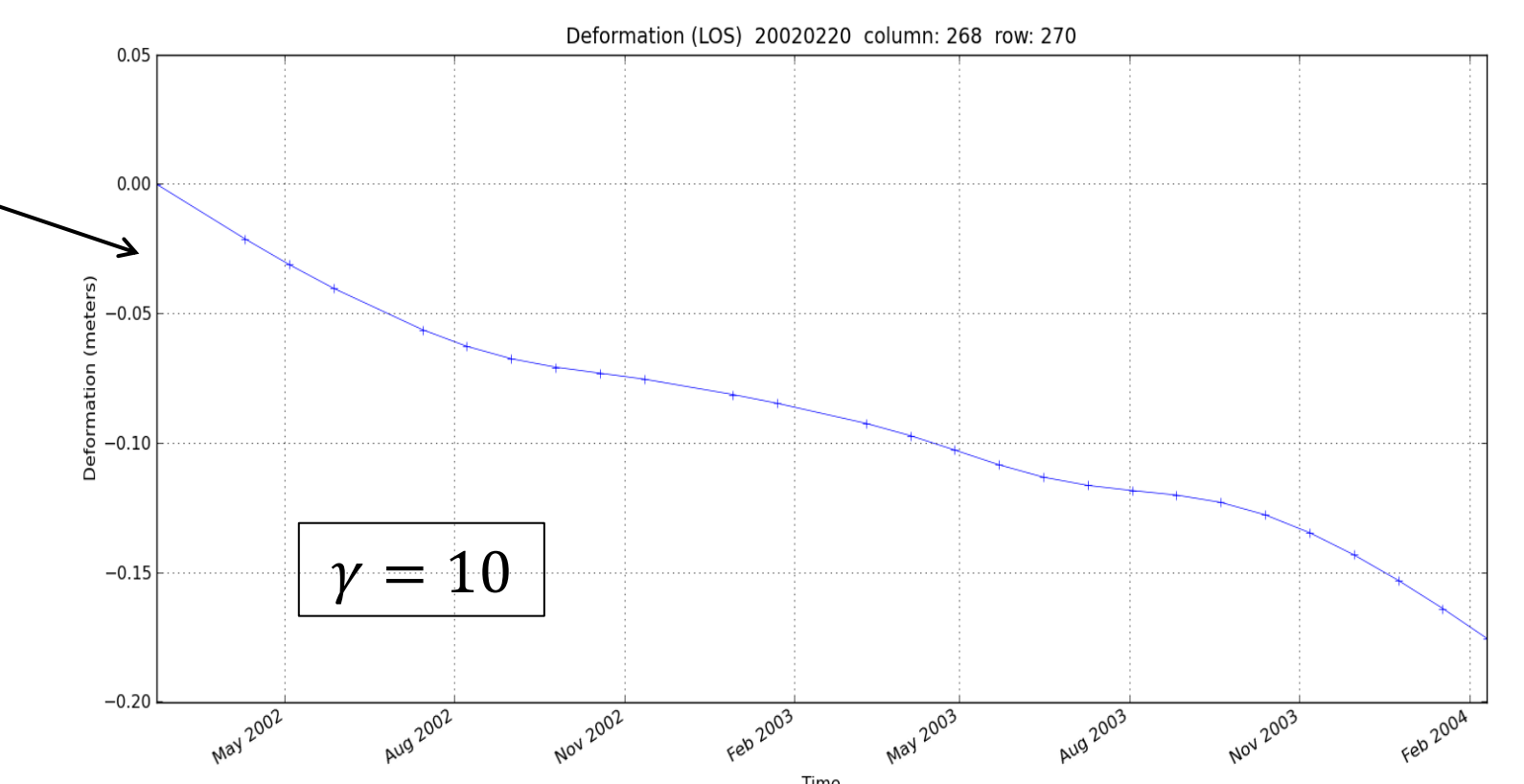
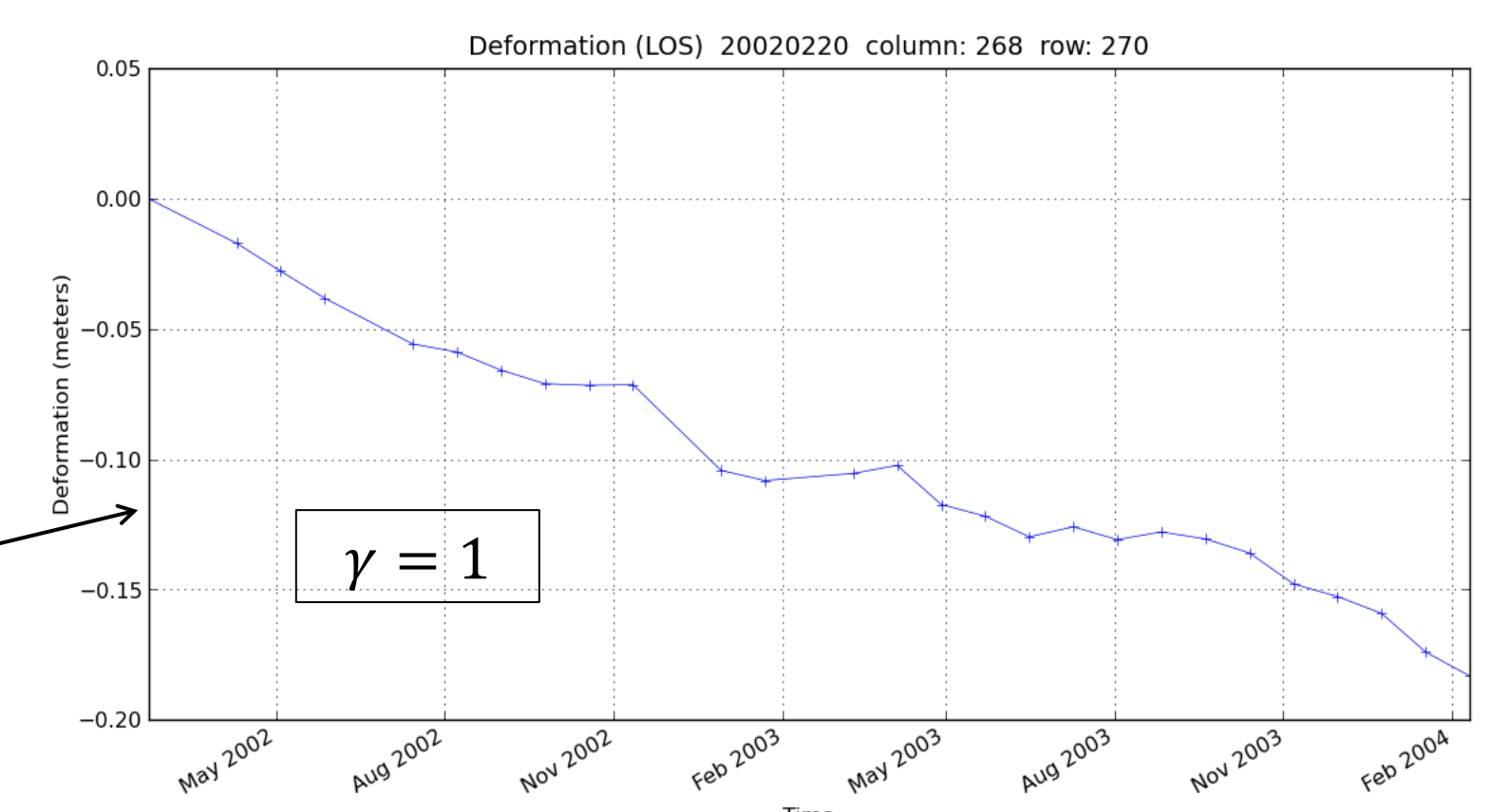


Figure 6. Height correction determined by SVD inversion of the differential interferometric phase, $\gamma = 1$.

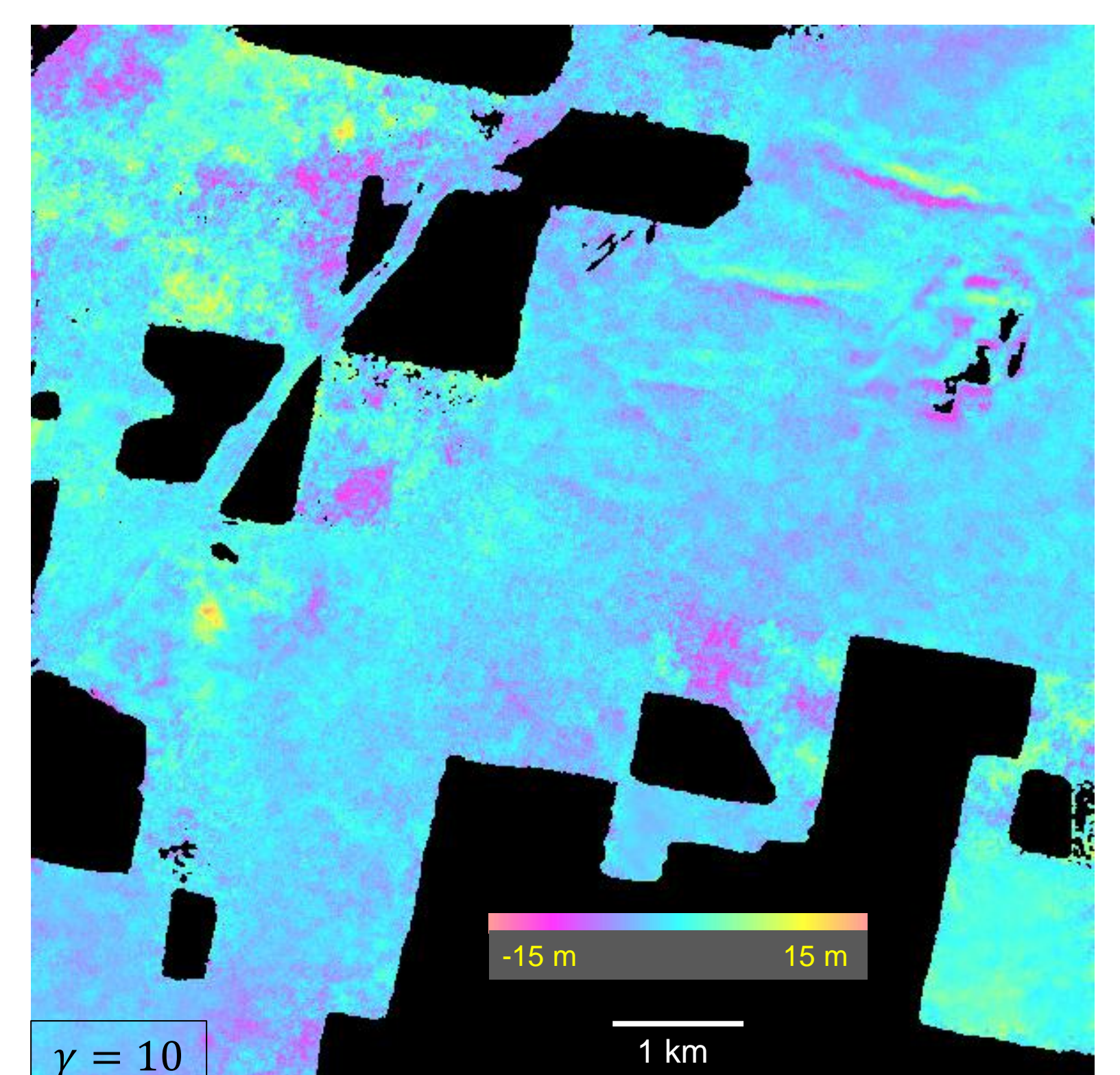


Figure 7. Height correction determined by SVD inversion of the differential interferometric phase, $\gamma = 10$.